Stereotactic and Functional Neurosurgery

Stereotact Funct Neurosurg , DOI: 10.1159/000553009
Received: October 31, 2025
Accepted: May 30, 2026
Published online: June 11, 2026

State-of-the-Art Imaging and Localization Assessment in Post-Operative Deep Brain Stimulation for Parkinson's Disease: A Review

Susanto KT, Premchand B, Wan KR, Yu W-Y, Oh HP, Chan VEY, Misbaah F, So RQ

ISSN: 1011-6125 (Print), eISSN: 1423-0372 (Online)
https://www.karger.com/SFN
Stereotactic and Functional Neurosurgery

Disclaimer:
Accepted, unedited article not yet assigned to an issue. The statements, opinions and data contained in this publication are solely those of the individual authors and contributors and not of the publisher and the editor(s). The publisher and the editor(s) disclaim responsibility for any injury to persons or property resulting from any ideas, methods, instructions or products referred to the content.

Copyright:
This article is licensed under the Creative Commons Attribution-NonCommercial 4.0 International License (CC BY-NC) (https://karger.com/Services/OpenAccessLicense). Usage and distribution for commercial purposes requires written permission.

© 2026 The Author(s). Published by S. Karger AG, Basel

Accepted Manuscript

Downloaded from http://karger.com/sfn/article-pdf/doi/10.1159/000553009/4547863/000553009.pdf by guest on 08 July 2026

State-of-the-Art Imaging and Localization Assessment in Post-Operative Deep Brain Stimulation for Parkinson's Disease: A Review

Kezia Tanesha Susanto [a, b], Brian Premchand [a], Kai Rui Wan [c, d], Wai-Yung Yu[e], Hui Ping Oh[e], Vincent Ern Yao Chan[e], Fatimah Misbaah [c, d], Rosa Qiyue So [a, b]

[a] Institute for Infocomm Research (I2R), Agency for Science, Technology and Research (A*STAR), 1 Fusionopolis Way, #21-01 Connexis (South Tower), Singapore 138632, Singapore
[b] Department of Biomedical Engineering, National University of Singapore, Singapore 117583, Singapore
[c] Department of Neurosurgery, National Neuroscience Institute, Tan Tock Seng Hospital, 11 Jalan Tan Tock Seng, Singapore 308433, Singapore
[d] Department of Neurosurgery, National Neuroscience Institute, Singapore General Hospital, Outram Road, Singapore 169608, Singapore
[e] Department of Neuroradiology, National Neuroscience Institute, Tan Tock Seng Hospital, Singapore, Singapore

Short Title: Post-operative Imaging and Localization of DBS in Parkinson's Disease

Corresponding Author:
Kezia Susanto
E-mail address:
stuks@a-star.edu.sg
Keywords: Parkinson's disease, deep brain stimulation, post-operative imaging, electrode localization, MRI, CT

Accepted Manuscript

Downloaded from http://karger.com/sfn/article-pdf/doi/10.1159/000553009/4547863/000553009.pdf by guest on 08 July 2026

Abstract

Background: Deep brain stimulation (DBS) is an established therapy for Parkinson's disease (PD), dependent on precise electrode placement relative to intended anatomical and functional targets. Post-operative imaging, primarily magnetic resonance imaging (MRI) and computed tomography (CT), is essential for verifying lead position, assessing surgical accuracy, and guiding stimulation programming.

Summary: Most centers perform imaging within the first week after surgery, typically using CT or MRI–CT fusion to confirm electrode location and detect complications. CT offers submillimeter resolution (slice thickness 0.5-1.25 mm; voxel ~0.5 mm) for clear electrode visualization, while MRI (particularly T1-MPRAGE, T2-FLAIR, and GRE sequences) provides superior anatomical contrast and artifact characterization.

Key Messages: Registration between pre- and post-operative scans remains the predominant localization technique, though automated pipelines such as Lead-DBS, Brainlab Elements™, SureTune4™ now achieve consistent precision within ±0.5–1.5 mm across platforms. This review summarizes current post-operative imaging strategies and quantitative localization techniques in DBS for PD. It discusses the advantages and limitations of each modality and outlines future directions in automation, multimodal integration, and personalized imaging pipelines for improving the accuracy, reproducibility, and clinical utility of post-operative DBS assessment.

Accepted Manuscript

Downloaded from http://karger.com/sfn/article-pdf/doi/10.1159/000553009/4547863/000553009.pdf by guest on 08 July 2026

Introduction

Deep brain stimulation (DBS) is a surgical therapy for advanced Parkinson's Disease (PD) that provides significant symptom relief by delivering high-frequency electrical stimulation to specific brain targets through implanted electrodes [1]. DBS electrodes typically target regions within the basal ganglia, most commonly the subthalamic nucleus (STN) or the globus pallidus internus (GPi) [2], [3], [4], [5]. A standard DBS lead consists of multiple contacts capable of monopolar or bipolar stimulation; more recent innovations include directional leads to improve targeting precision and reduce side effects [6]. One common targeting workflow includes pre-op planning, intra-op recording, and post-op imaging confirmation. A critical aspect of successful DBS therapy lies in the accuracy of electrode placement and the fine-tuning of stimulation parameters, both of which rely heavily on imaging [7]. Post-operative imaging plays an important role in confirming lead placement relative to intended targets, identifying surgical complications, and guiding individualized programming to optimize clinical benefit.

Several prior reviews have examined imaging in DBS from complementary perspectives. Saleh et al. (2016) provided an early focused overview of post-operative imaging in DBS, discussing CT and MRI modalities, safety considerations, and methodological challenges, and highlighting the lack of standardization in post-operative imaging practice [8]. Since that publication, however, post-operative DBS imaging has evolved substantially, with advances in acquisition protocols, higher-field MRI, improved CT resolution, and the increasing use of automated and atlas-based localization pipelines in both research and clinical workflows. Boutet et al. reviewed the broader role of neuroimaging in neuromodulation, emphasizing network-level mechanisms and functional imaging approaches rather than post-op localization pipelines [9]. Peng et al. provided a comprehensive overview of neuroimaging techniques applied across neurodegenerative and neuropsychiatric disorders but did not focus on post-operative DBS electrode localization accuracy or reproducibility [10]. Reviews by van den Munckhof et al. and Singh et al. focused primarily on surgical targeting strategies and operative techniques, with less emphasis on post-implantation imaging workflows [2], [11]. Xiao et al. offered an extensive review of image guidance in DBS surgery, largely centered on intra-operative navigation and targeting [12], while Moraes de Falcone et al. discussed imaging in the context of suboptimal DBS parameters [13]. Despite these contributions, there is a need for an updated synthesis that reflects present-day post-operative imaging practices, including modern MRI and CT acquisition protocols, multimodal fusion strategies, and software-based localization workflows now commonly used to support DBS programming and outcome interpretation in Parkinson's disease.

This review aims to clarify current standards of post-operative DBS imaging, identify sources of localization error, and discuss emerging strategies to improve reproducibility and clinical translation. In doing so, it seeks to provide a practical framework for optimizing post-operative DBS assessment and supporting more precise, personalized therapy in Parkinson's disease.

Methods

A structured literature search was conducted to identify peer-reviewed studies on post-operative imaging for DBS in PD, with emphasis on lead-localization accuracy and imaging-based verification.

Search Strategy and Databases

Literature searches were performed in PubMed and Scopus, covering publications from January 2015 to December 2025. PubMed was selected for its comprehensive coverage of biomedical and clinical neuroscience literature through MEDLINE and use of controlled vocabulary (MeSH), and Scopus was included to complement PubMed by capturing interdisciplinary and technical publications, making both well suited for identifying clinically relevant DBS and neuroimaging studies, computational pipelines, as well as engineering-focused DBS research that may not be indexed in MEDLINE.

Search terms were combined using Boolean operators and included variations of: *("Parkinson Disease" OR "Parkinson's Disease") AND ("Deep Brain Stimulation" OR DBS) AND (postoperative OR post-operative OR post-surgical) AND (imaging OR MRI OR magnetic resonance imaging OR CT OR*

Downloaded from http://karger.com/sfn/article-pdf/doi/10.1159/000553009/4547863/000553009.pdf by guest on 08 July 2026

computed tomography OR DTI OR diffusion OR tractography OR neuroimaging) AND (localization OR localisation OR registration OR fusion OR lead placement OR electrode position OR trajectory OR accuracy OR reconstruction). Representative search queries results for each database are provided in the Supplementary Material.

The search timeframe was restricted to the past 10 years to reflect contemporary DBS practice, as advances in imaging resolution, lead design, multimodal fusion, and automated localization software have altered or improved post-operative workflows. Thus, this review aims to synthesize current and clinically relevant approaches.

Eligibility Criteria

Eligibility criteria (listed in Table 1) were defined a priori to ensure methodological rigor and relevance to post-operative imaging-based DBS localization in Parkinson's disease. Reference lists of relevant review articles and key primary studies were manually screened to identify additional eligible publications.

Study Selection and Screening

This review addresses the following question: *In patients with Parkinson's disease undergoing DBS, how do different post-operative imaging modalities and localization pipelines (MRI, CT, and fusion-based approaches) compare in terms of electrode localization accuracy, reproducibility, and clinical utility?* The population of interest comprises PD patients implanted with DBS electrodes. The interventions include post-operative imaging and localization approaches together with quantitative and automated pipelines. Comparisons are made across imaging modalities, fusion strategies, and localization methods. Outcomes of interest include localization accuracy and precision, robustness across platforms, and relevance for programming, complication detection, and interpretation of clinical response.

Database searches identified 330 records. After removal of 59 duplicates, 271 records underwent title screening. Abstract screening resulted in exclusion studies focused on perioperative complications (pneumocephalus, edema, hemorrhage, anesthesia comparisons; n=22), MER physiology or surgical positioning alone (n=14), cognitive or radiomic delirium studies and ablative procedures (n=20), and non-imaging clinical outcomes such as gait, psychiatric symptoms, or quality of life (n=14). This process yielded 201 records for full-text assessment. Of these, 1 article was excluded due to language, and 129 were excluded for lack of relevance to post-operative imaging localization or programming. A final set of 71 studies was included for qualitative synthesis.

Due to substantial heterogeneity in imaging protocols, analytical methods, and outcome reporting, a meta-analysis was not feasible. Instead, findings were synthesized narratively. Included studies were categorized into six thematic groups: review articles (*n* = 7), localization accuracy studies (*n* = 23), software and pipeline development (*n* = 14), diffusion imaging and connectomics (*n* = 11), imaging modality-focused studies (*n* = 11), and programming optimization studies (*n* = 5). The study selection process (using the PRISMA 2020 guidelines [14]) and thematic distribution are summarized in Fig. 1. a and Fig. 1. b, respectively.

Imaging Modalities in Post-Operative DBS Assessment

In addition to standard post-operative diagnostic computed tomography (CT) to rule out hemorrhage, imaging practices have now expanded to include thin cut CT after DBS surgery to confirm lead placement [15]. Nowadays, practices used vary from CT-only approaches to immediate magnetic resonance imaging (MRI), or combined modalities with image fusion (MRI and CT) [16]. The main modalities employed after DBS surgery to visualize electrode location and brain anatomy include MRI, CT, and MRI–CT fusion.

Magnetic Resonance Imaging (MRI)

Magnetic resonance imaging (MRI) visualizes internal brain structures by detecting the magnetic properties of hydrogen nuclei in water and fat, producing high-contrast, three-dimensional images that are ideal for assessing deep brain targets after DBS surgery [17]. MRI is considered the gold standard for anatomical localization of DBS leads as its excellent soft tissue contrast allows direct

Accepted Manuscript

Downloaded from http://karger.com/sfn/article-pdf/doi/10.1159/000553009/4547863/000553009.pdf by guest on 08 July 2026

visualization of targets like the STN or GPi and surrounding anatomy, which is used for confirming that electrodes are correctly positioned [18], [19], [20]. MRI can reveal the artifact of the DBS lead within the brain, as well as any edema or micro hemorrhages induced by surgery [21], [22]. Specialized MRI sequences can improve the visualization of both the electrode and target. For example, Li et al. (2021) recommend a protocol combining 3D T1-weighted MRI (MPRAGE), T2 spin-echo, and multi-echo gradient echo (GRE) to map the brain and the implanted electrodes, noting this provided excellent pre- and post-operative visualization of the brain targets and electrodes [23]. T1-weighted and T2-weighted images offer complementary information: T1 images suffer less geometric distortion from the hardware, whereas T2 images (especially T2*-weighted GRE) highlight iron-rich nuclei like the STN with better contrast [24]. Newer MRI methods, such as susceptibility-weighted imaging (SWI), further improve visualization of deep brain targets (the STN is more visible on SWI) but may not be ideal for seeing the electrode contacts due to blooming artifact [25], [26], [27]. Fluid-attenuated inversion recovery (FLAIR) can enhance visualization of the subthalamic nucleus compared with T2 sequences [28], and is useful for detecting perielectrode edema post-operatively. However, its geometric distortion and blurred artifacts limit accuracy for electrode localization [29]. Previously, the major consideration was safety because of MRI-related heating risks. Modern studies, however, have shown that MRI at 1.5T or 3T can be performed safely in patients with implanted DBS systems if strict protocols, such as limiting specific absorption rate, proper device settings, etc., are followed [30], [31]. Notably, Nuzov et al. (2023) demonstrated in a phantom study that the MR artifact can mislead localization, the actual DBS lead tip was consistently a few millimeters beyond the artifact's tip on MRI, with the gap varying by sequence and orientation (up to 4.99 mm) [32]. Additionally, MRI lacks the capability to provide orientation information about the directional lead [33]. Nevertheless, MRI is a powerful tool for post-operative DBS evaluation, but it must be used with techniques to mitigate artifact and under safe scanning practices.

Computed Tomography (CT)

CT imaging is widely used in the immediate post-operative period for DBS lead localization and complication screening [8]. CT has several advantages: it has minimal geometric distortion, even in the presence of the metal electrode, and shows the lead as a bright hyperdense object that can be readily identified in stereotactic space. This makes CT highly reliable for determining electrode coordinates. In fact, a prospective study by Kremer et al. (2019) found that intraoperative CT was non-inferior to MRI for determining DBS lead tip location, with an average difference of 1 mm between CT and MRI measurements of lead position [34]. CT is fast (a head CT takes only minutes) and avoids any MRI-related risks, making it suitable for patients who cannot undergo MRI due to device or medical constraints.

However, its lack of soft-tissue contrast means the brain target (e.g. STN) is not directly shown on CT. In addition, metallic DBS leads can generate streak artifacts caused by proton starvation and beam hardening, which may degrade image quality and obscure surrounding structures. Artifact-reduction techniques such as the single-energy metal artifact reduction (SEMAR) algorithm have been shown to reduce these streaks and improve visualization [35]. CT also involves ionizing radiation exposure, though a single head CT is a relatively low dose at around 2 millisievert [36], [37]. Another drawback is that CT is less sensitive than MRI for small hemorrhages or edema along the electrode track, these often appear only as subtle changes or may be missed on CT, whereas MRI can detect dozens of tiny microhemorrhages [29]. Fig. 2 shows representative MRI and CT images from example patients showing pre-op T1-weighted MRI, post-op CT, T1- and T2-weighted MRI scans.

MRI–CT Fusion

Post-operative CT combined with MRI enables a comprehensive view of both the electrode location and the surrounding anatomical targets such as the STN and GPi. The most common workflow involves fusing pre-operative MRI (typically T1-weighted for anatomical definition) with post-operative CT [38], [39]. This fusion approach leverages the complementary strengths of both

Accepted Manuscript

Downloaded from http://karger.com/sfn/article-pdf/doi/10.1159/000553009/4547863/000553009.pdf by guest on 08 July 2026

modalities, CT's precise depiction of hardware and MRI's superior soft-tissue contrast, to determine the exact electrode position relative to intended targets.

However, several sources of localization error must be considered. Registration inaccuracies during MRI–CT co-alignment can introduce errors of up to 1–2 mm, depending on voxel size, patient movement, and software algorithms used [40], [41]. Brain shift, caused by cerebrospinal fluid loss or postoperative edema, can further distort correspondence between pre- and post-operative datasets, and longitudinal changes may alter electrode-target relationships over time [42], [43].

Quantitative Localization Pipelines

Post-operative DBS localization in PD is now dominated by semi-automated quantitative pipelines that typically perform these core steps: (i) co-register post-op CT and/or MRI to pre-op MRI, (ii) reconstruct the lead trajectory and contact coordinates, (iii) quantify distance/angle to intended targets, and (iv) optionally estimate electric-field/VTA for programming.

The open-source Lead-DBS suite (https://www.lead-dbs.org), widely adopted in research (and not licensed for direct clinical use), implements robust CT/MRI registration, artifact-based lead reconstruction, brain-shift correction utilities, MNI non-linear normalization, and electric field/volume of tissue activated (VTA) modeling with atlas/tract overlays [44], [45], [46]. These features have enabled large-scale, cross-cohort analyses linking contact location to clinical outcomes and adverse effects. In parallel, commercial platforms such as Brainlab Elements™, Medtronic SureTune™, and Boston Scientific Illumina™ provide integrated fusion, automated contact picking, and similarly VTA visualization [47]. Research-oriented frameworks such as StimVision focus on pathway-specific activation (e.g., hyperdirect or pallidothalamic tracts) to relate contact location and stimulation settings to putative network mechanisms [48]. PaCER (Post-operative CT Electrode Reconstruction) enables fully automated lead reconstruction from CT data and is particularly relevant in the presence of brain shift or subtle electrode curvature [49]. Unlike straight-line fitting approaches, PaCER models the electrode shaft as a smooth, curved trajectory derived from the CT artifact profile. This allows reliable detection of individual contacts even when bending occurs. In head-to-head evaluations, inter-software variability is measurable but generally sub-millimetric to low-millimetric: in 105 PD patients, Lead-DBS, SureTune4™, and Brainlab Elements™ showed Euclidean distance differences for active-contact localization on the order of ~0.5-1.5 mm, with additional analyses of VTA overlap and operator repeatability [47]. Concordance between intra-op MRI and early post-op CT localizations is also high, with trajectory errors on average < 1 mm, although disagreement increases with longer durations due to migration/brain shift [50]. Across pipelines, the common workflow is: CT-MRI fusion to exploit CT's crisp electrode depiction and MRI's anatomical contrast; extraction of contact centroids and shaft vectors; computation of 3-D coordinates/angles relative to surgical plan and atlas space to report deviation to motor STN/GPi; and VTA simulation linked to atlases/tractography for image-guided programming [44], [46], [51].

Imaging and Localization Protocols Reported in Previous Studies

The acquisition parameters and imaging protocols used across previous studies are summarized in Table 2, illustrating the diversity of MRI and CT settings adopted for accurate DBS lead localization and fusion-based analysis. Most studies acquire post-operative images within 24 hours to one week after surgery, primarily for lead verification and safety assessment. CT and MRI–CT fusion remain standard in many centers, as CT provides clear electrode visualization while MRI adds anatomical and soft-tissue context. Reported CT parameters typically include slice thicknesses of 0.5-1.25 mm and in-plane resolution near 0.5 mm. For MRI, common sequences are T1-weighted MPRAGE (0.45-1 mm), T2-FLAIR, and GRE or T2* sequences for artifact mapping, with 3 T scanners increasingly preferred over 1.5 T systems for improved grey-white contrast and reduced voxel size. Based on reported localization errors and target dimensions, a practical lower bound for reliable lead localization is a CT slice thickness 1.0 mm and MRI voxel size 1.0 mm isotropic. Resolutions coarser than this approach the scale of clinically meaningful subterritorial differences within the STN or GPi, increasing uncertainty in contact-to-target assignment and subsequent programming decisions. In terms of

Downloaded from http://karger.com/sfn/article-pdf/doi/10.1159/000553009/4547863/000553009.pdf by guest on 08 July 2026

localization methods, rigid registration (aligning images using translation and rotation without deformation) between pre- and post-operative scans remains the most widely used approach, but automated pipelines such as Lead-DBS, Brainlab Elements™, SureTune4™, PaCER, DBSproc, and ESM-CT have standardized electrode localization with typical precision between 0.5 and 1.5 mm. Emerging techniques such as ultrasound-assisted localization by Reese et al. showed comparable submillimeter accuracy (0.32 ± 0.87 mm difference compared to MRI-based results) while avoiding radiation exposure [52].

Post-Operative Imaging and Localization Roles in DBS Optimization

Post-operative imaging plays a pivotal role in optimizing DBS for PD by confirming lead accuracy, correlating electrode position with clinical outcomes, and detecting complications. It is crucial to accurately localize the electrode relative to its intended target, as even millimeter-scale deviations can significantly alter therapeutic benefit or side-effect thresholds.

Quantitative pipelines such as those by Husch et al. (2018) integrate post-op imaging with high-field atlases to generate 3D maps and reports showing contact positions relative to subcortical nuclei, supporting early identification of misplaced leads and guiding potential re-operation or contact selection [53]. Large cohort analyses further demonstrated that spatial proximity to sensorimotor STN or posteroventral GPi is strongly associated with motor improvement, whereas off-target placement increases the likelihood of capsular or limbic side effects [54], [55], [56], [57].

Imaging findings also directly inform clinical programming and outcome interpretation. Several studies demonstrate that electrodes positioned within the dorsolateral sensorimotor STN correlate with superior improvement in PD symptoms [54], [58], [59]. Imaging-based reports or software visualizations now routinely assist clinicians during programming by highlighting which contacts lie closest to the intended territory [60]. This reduces trial-and-error during parameter adjustment and helps explain unexpected outcomes, such as limited benefit from off-target placement or stimulation near non-motor pathways. These tools are particularly valuable in complex cases involving directional leads, atypical anatomy, or mixed symptom profiles.

Finally, post-operative imaging is critical for detecting surgical or stimulation-related complications [61]. Early CT or MRI can reveal haemorrhage, oedema, or pneumocephalus before symptoms develop. In a cohort of 198 patients, Succop et al. (2023) found that 6% had intracranial hematomas and over one-third showed small microhaemorrhages along the electrode tract, findings that were more frequent after multiple microelectrodes pass but largely asymptomatic [29]. Imaging also enables identification of lead migration, which occurs in up to 10% of cases and can diminish long-term efficacy [62].

Challenges in Imaging and Localization

Despite advances in imaging technology and software, several challenges continue to limit the precision and reliability of post-operative DBS localization. Imaging artifacts remain a major concern: metallic components of the DBS lead produce susceptibility and blooming artifacts on MRI, often obscuring the true contact position, while streak artifacts can occur on CT though usually without masking the electrode tip [32]. These distortions hinder accurate lead reconstruction and can affect tractography near the electrode, as fibre tracts passing adjacent to the signal void may not be resolved [63].

A growing concern in post-operative DBS imaging is not only variability in acquisition but the chain of registration errors that propagate through the localization workflow. Each computational step (coregistering post-op CT to pre-op MRI, normalizing images to atlas space, and reconstructing the lead trajectory) introduces small but cumulative errors that can collectively shift the estimated contact position within the compact STN. Lead-DBS, Brainlab Elements™, and SureTune™ use varying normalization routines and artifact models; as a result, reconstructed lead positions can diverge by up to several millimeters when applied to the same dataset. Moreover, these pipelines often rely on non-linear normalization to standard MNI space and atlas-based connectivity rather than fully individualized diffusion data, which may not perfectly capture each patient's unique subcortical

Downloaded from http://karger.com/sfn/article-pdf/doi/10.1159/000553009/4547863/000553009.pdf by guest on 08 July 2026

anatomy, especially in brains affected by disease or age-related atrophy. There is currently no universally accepted *ground truth* for post-operative DBS localization.

One potential strategy to mitigate these uncertainties is the use of physical or digital phantoms with known electrode geometries, which can provide reference standards for validating reconstruction algorithms, registration accuracy, and inter-software variability. Phantom-based benchmarking has been proposed as a means to disentangle true anatomical uncertainty from software-induced error [49], [64], but remains underutilized in routine validation of clinical and research pipelines.

Another challenge is dynamic post-operative change, including intra-operative brain shift, postoperative oedema, and gradual tissue remodelling, can alter the electrode-target relationship over time [65], [66], [67]. Pneumocephalus is frequent after DBS and can be associated with measurable brain shift that perturbs electrode-target correspondence during early recovery. In staged DBS cohorts, pneumocephalus has been reported in the majority of patients (84%), with mean brain-shift on the order of ~0.8 mm, even when lead shift is smaller on average [43]. Over longer intervals, tissue healing and tethering along the extracranial course can transmit tension to the intracranial lead, contributing to delayed migration. In a large serial-CT localization cohort (138 leads), >3 mm delayed migration occurred in 12.3% of leads (12.1% of patients), a magnitude that can change contact selection, therapeutic window, and side-effect thresholds [68].

In addition to meticulous surgical technique, strategies to reduce error associated with brain shift include minimizing the interval between surgery and imaging (immediately after surgery or within a day), preferential use of early intra-operative, application of brain-shift correction algorithms [42], [46], and selective use of longitudinal imaging when clinical response deviates from expectations. However, systematic guidelines on when repeat imaging is needed remain lacking. Addressing these challenges will require harmonized imaging standards, validation frameworks, and tighter integration between radiological and clinical workflows.

Future Directions and Emerging Technologies

Connectomic imaging and diffusion MRI

Diffusion MRI and tractography now extend post-operative imaging beyond anatomy to network-level analysis. By mapping white-matter tracts near the electrode, such as the hyperdirect and dentatorubrothalamic pathways, researchers can relate the volume of tissue activated (VTA) to patient-specific connectivity profiles [63], [69]. Recent large-cohort work has strengthened this approach: Rajamani et al. (2024) demonstrated that stimulation of symptom-specific white-matter tracts predicted differential improvements across PD symptoms [70], while Abe et al. (2024) showed that tractography could forecast DBS-induced network effects across patients [71]. As diffusion modelling and artifact correction continue to improve, post-operative DTI is increasingly feasible for clinical use [72]. It can serve as a verification and programming aid, identifying which fibre pathways are effectively modulated by stimulation. However, tractography-derived results remain sensitive to choices in methodology, including deterministic versus probabilistic reconstruction algorithms, user-defined region-of-interest (ROI) selection, and software-specific implementations [73]. Different versions of commercial platforms support varying levels of diffusion processing, which may further contribute to inter-software variability. Future progress will depend on standardizing DTI acquisition parameters, refining distortion correction, and testing the clinical utility of integrating tractography into surgical planning and post-operative platforms [74], [75], [76]. Connectomic imaging may soon transition to a clinically actionable component of personalized DBS programming, directly linking stimulation networks to symptom-specific outcomes [77].

Image Fusion Strategies

Beyond conventional CT–MRI fusion, alternative image-fusion strategies are emerging as MRI quality and artifact-mitigation techniques improve. Several studies suggest that MRI–MRI fusion, when pre- and post-operative scans are acquired with identical geometry and sequence parameters, may offer modest gains in anatomical consistency by minimizing cross-modality contrast differences and registration uncertainty [78]. This approach is particularly attractive as optimized MRI sequences and

Accepted Manuscript

Downloaded from http://karger.com/sfn/article-pdf/doi/10.1159/000553009/4547863/000553009.pdf by guest on 08 July 2026

reconstruction methods increasingly allow visualization of DBS leads despite susceptibility artifacts. However, MRI-only workflows remain constrained by residual artifact variability, safety considerations, and limited reliability in resolving directional lead orientation. In contrast, CT–CT fusion, such as alignment of early and delayed post-operative CT scans, offers high geometric fidelity and is well suited for longitudinal assessment of lead migration or rotation, where relative positional change rather than anatomical targeting is the primary objective [50], [79]. The absence of soft-tissue contrast, however, limits its utility for target-based localization and programming guidance, positioning CT–CT as a complementary rather than standalone strategy.

Looking ahead, ultra-high-field MRI (7T) holds promise for advancing MRI-only localization workflows by offering substantially improved spatial resolution and subcortical contrast, potentially enabling more precise visualization of DBS targets and lead–tissue relationships [80], [81]. As access to 7T systems expands and safety protocols mature, MRI-based localization may play a larger role in selected centers. Systematic benchmarking across fusion strategies will be essential to determine when these advances translate into meaningful benefits in DBS programming and outcomes.

AI-assisted localization and auto-segmentation

Deep-learning algorithms are being developed to automate electrode detection, segmentation, and labelling in CT/MRI, reducing operator variability and analysis time [82]. Neudorfer et al. (2023) introduced end-to-end electrode localization algorithms within Lead-DBS version 3 that provide reproducible coordinate extraction and visualization [44], while Rolland et al. (2024) demonstrated automated image-guided programming in clinical workflows [83]. An emerging direction involves combining imaging-based localization with intraoperative electrophysiology, particularly microelectrode recordings (MER), to achieve more precise mapping of lead trajectories and target boundaries. Recent developments from Bergman and colleagues using Alpha Omega systems have demonstrated the feasibility of synchronizing MER signals with imaging data, creating hybrid anatomical-functional maps that can verify electrode placement relative to physiological landmarks. Such integration could bridge the gap between structural imaging and real-time electrophysiological confirmation, supporting fully automated localization pipelines for clinical DBS applications [84].

Personalized programming

Modern imaging and modelling are shifting DBS programming toward a predictive and personalized approach. By combining MRI, CT, diffusion tractography, and intraoperative data within standardized pipelines, clinicians can map electrode positions relative to patient-specific anatomical and functional targets [44], [85].

Emerging AI tools now link imaging features with clinical outcomes to recommend optimal contacts and stimulation settings. For example, Rajamani et al. (2024) showed that targeting white-matter tracts specific to tremor, rigidity, or bradykinesia improves symptom relief and reduces side-effect risk [70]. In a complementary vein, the paper by Roediger et al. (2023) evaluated an imaging-based algorithm that uses patient-specific imaging data to suggest programming settings automatically [86]. The goal is a tailored programming strategy based on anatomy, connectivity, and symptom profile rather than fixed target coordinates.

Conclusion

Post-operative imaging remains essential for verifying electrode placement and optimizing clinical outcomes in deep brain stimulation for Parkinson's disease. Advances in high-resolution MRI, precise CT acquisition, and multimodal fusion have improved localization accuracy to the submillimeter range. Automated pipelines such as Lead-DBS and Brainlab Elements™ have standardized analysis, while AI-driven segmentation and tractography are beginning to personalize lead assessment. Recent studies integrating post-operative imaging with clinical outcomes have shown that symptom-specific targeting and predictive algorithms can refine stimulation parameters and reduce side effects. The convergence of imaging, modelling, and automation now points toward a future of data-driven, patient-specific programming, where DBS therapy is optimized not only by anatomical precision but also by individual connectivity and symptom profile. Broader standardization of post-operative

Accepted Manuscript

Downloaded from http://karger.com/sfn/article-pdf/doi/10.1159/000553009/4547863/000553009.pdf by guest on 08 July 2026

imaging protocols, localization workflows, and reporting metrics is needed to enable meaningful comparison across institutions and implantation strategies.

Accepted Manuscript

Downloaded from http://karger.com/sfn/article-pdf/doi/10.1159/000553009/4547863/000553009.pdf by guest on 08 July 2026

Statements

Conflict of Interest Statement

The authors have no conflicts of interest to declare.

Funding Sources

This research is supported by Singhealth Duke Academic medicine research grant (Artificial Intelligence) AM/AIR011/2022 (SRDUKAMR22A1) for the Deep Brain Stimulation project. The projects are done and supported by the Institute for Infocomm Research (I^2R), Agency for Science, Technology and Research (A*STAR) Singapore, and the Singapore International Graduate Award (SINGA), A*STAR Graduate Academy (A*GA). The funders of the study had no role in study design, data collection, data analysis, data interpretation, or writing of the report. The author had full access to all the data in the study and had overall responsibility for the decision to submit for publication. No funding was received from the drug manufacturer or distributor.

Author Contributions

K.S. performed data curation, formal analysis, investigation, visualization, and writing of the original draft. F.M. assisted with data curation for the MRI and CT figures in this manuscript. Y.W.Y, O.H.P, and V.C.E.Y. assisted with visualization, manuscript review and editing. B.P., K.R.W., and R.Q.S. contributed to conceptualization, supervision, and manuscript review and editing.

Accepted Manuscript

Downloaded from http://karger.com/sfn/article-pdf/doi/10.1159/000553009/4547863/000553009.pdf by guest on 08 July 2026

References

[1] A. L. Benabid, S. Chabardes, J. Mitrofanis, and P. Pollak, "Deep brain stimulation of the subthalamic nucleus for the treatment of Parkinson's disease," *Lancet Neurol.*, vol. 8, no. 1, pp. 67–81, Jan. 2009, doi: 10.1016/S1474-4422(08)70291-6.

[2] P. van den Munckhof, M. Bot, and P. R. Schuurman, "Targeting of the Subthalamic Nucleus in Patients with Parkinson's Disease Undergoing Deep Brain Stimulation Surgery.," *Neurol. Ther.*, vol. 10, no. 1, pp. 61–73, Jun. 2021, doi: 10.1007/s40120-021-00233-8.

[3] S. J. Groiss, L. Wojtecki, M. Südmeyer, and A. Schnitzler, "Deep brain stimulation in Parkinson's disease.," *Ther. Adv. Neurol. Disord.*, vol. 2, no. 6, pp. 20–8, Nov. 2009, doi: 10.1177/1756285609339382.

[4] J. Voges *et al.*, "Bilateral high-frequency stimulation in the subthalamic nucleus for the treatment of Parkinson disease: correlation of therapeutic effect with anatomical electrode position," *J. Neurosurg.*, vol. 96, no. 2, pp. 269–279, Feb. 2002, doi: 10.3171/jns.2002.96.2.0269.

[5] J. Herzog *et al.*, "Most effective stimulation site in subthalamic deep brain stimulation for Parkinson's disease," *Mov. Disord.*, vol. 19, no. 9, pp. 1050–1054, Sep. 2004, doi: 10.1002/mds.20056.

[6] F. Steigerwald, C. Matthies, and J. Volkmann, "Directional Deep Brain Stimulation," *Neurotherapeutics*, vol. 16, no. 1, pp. 100–104, Jan. 2019, doi: 10.1007/s13311-018-0667-7.

[7] A. Wagle Shukla, P. Zeilman, H. Fernandez, J. A. Bajwa, and R. Mehanna, "DBS Programming: An Evolving Approach for Patients with Parkinson's Disease.," *Park. Dis.*, vol. 2017, p. 8492619, 2017, doi: 10.1155/2017/8492619.

[8] C. Saleh, G. Dooms, C. Berthold, and F. Hertel, "Post-operative imaging in deep brain stimulation: A controversial issue," *Neuroradiol. J.*, vol. 29, no. 4, pp. 244–249, Aug. 2016, doi: 10.1177/1971400916639960.

[9] A. Boutet, J. Germann, and A. Fasano, "Imaging and neuromodulation in Parkinson's disease," *Curr. Opin. Neurol.*, 2025, doi: 10.1097/WCO.0000000000001380.

[10] S. Peng, V. Dhawan, D. Eidelberg, and Y. Ma, "Neuroimaging evaluation of deep brain stimulation in the treatment of representative neurodegenerative and neuropsychiatric disorders," *Bioelectron. Med.*, vol. 7, no. 1, p. 4, Mar. 2021, doi: 10.1186/s42234-021-00065-9.

[11] M. Singh, K. V. Shabari Girishan, J. Bajaj, and K. Garg, "Deep brain stimulation for movement disorders: Surgical nuances," *Neurol. India*, vol. 66, no. 7, pp. S122–S130, 2018, doi: 10.4103/0028-3886.226461.

[12] Y. Xiao, J. C. Lau, D. Hemachandra, G. Gilmore, A. R. Khan, and T. M. Peters, "Image Guidance in Deep Brain Stimulation Surgery to Treat Parkinson's Disease: A Comprehensive Review," *IEEE Trans. Biomed. Eng.*, vol. 68, no. 3, pp. 1024–1033, Mar. 2021, doi: 10.1109/TBME.2020.3006765.

[13] A. C. Moraes De Falcone, C. França, T. G. Guimarães, and R. G. Cury, "The electric brain: approach to suboptimal DBS parameters," *Clin. Park. Relat. Disord.*, vol. 14, p. 100418, 2026, doi: 10.1016/j.prdoa.2025.100418.

[14] M. J. Page *et al.*, "The PRISMA 2020 statement: an updated guideline for reporting systematic reviews," *BMJ*, p. n71, Mar. 2021, doi: 10.1136/bmj.n71.

[15] D. Servello, E. Zekaj, C. Saleh, C. Pacchetti, and M. Porta, "The pros and cons of intraoperative CT scan in evaluation of deep brain stimulation lead implantation: A retrospective study," *Surg. Neurol. Int.*, vol. 7, no. 20, p. 551, 2016, doi: 10.4103/2152-7806.187534.

[16] J. Xia, P. He, X. Cai, D. Zhang, and N. Xie, "Magnetic resonance and computed tomography image fusion technology in patients with Parkinson's disease after deep brain stimulation," *J. Neurol. Sci.*, vol. 381, pp. 250–255, Oct. 2017, doi: 10.1016/j.jns.2017.08.3267.

[17] A. Berger, "Magnetic resonance imaging," *BMJ*, vol. 324, no. 7328, p. 35, Jan. 2002, doi: 10.1136/bmj.324.7328.35.

[18] C. Pollo *et al.*, "Localization of electrodes in the subthalamic nucleus on magnetic resonance imaging," *J. Neurosurg.*, vol. 106, no. 1, pp. 36–44, Jan. 2007, doi: 10.3171/jns.2007.106.1.36.

[19] J. A. Hyam, H. Akram, T. Foltynie, P. Limousin, M. Hariz, and L. Zrinzo, "What You See Is What You Get," *Oper. Neurosurg.*, vol. 11, no. 3, pp. 412–419, Sep. 2015, doi: 10.1227/NEU.0000000000000848.

[20] X. Liu, J. Zhang, K. Fu, R. Gong, J. Chen, and J. Zhang, "Microelectrode Recording–Guided Versus Intraoperative Magnetic Resonance Imaging–Guided Subthalamic Nucleus Deep Brain Stimulation Surgery for Parkinson Disease: A 1-Year Follow-Up Study," *World Neurosurg.*, vol. 107, pp. 900–905, Nov. 2017, doi: 10.1016/j.wneu.2017.08.077.

Downloaded from http://karger.com/sfn/article-pdf/doi/10.1159/000553009/4547863/000553009.pdf by guest on 08 July 2026

[21] A. J. Martin, P. A. Starr, J. L. Ostrem, and P. S. Larson, “Hemorrhage Detection and Incidence during Magnetic Resonance-Guided Deep Brain Stimulator Implantations,” *Stereotact. Funct. Neurosurg.*, vol. 95, no. 5, pp. 307–314, 2017, doi: 10.1159/000479287.
[22] C. M. Matias, L. A. Frizon, F. Asfahan, J. D. Uribe, and A. G. Machado, “Brain Shift and Pneumocephalus Assessment During Frame-Based Deep Brain Stimulation Implantation With Intraoperative Magnetic Resonance Imaging,” *Oper. Neurosurg.*, vol. 14, no. 6, pp. 668–674, Jun. 2018, doi: 10.1093/ons/opx170.
[23] Y. Li *et al.*, “Imaging patients pre and post deep brain stimulation: Localization of the electrodes and their targets,” *Magn. Reson. Imaging*, vol. 75, pp. 34–44, Jan. 2021, doi: 10.1016/j.mri.2020.09.016.
[24] E. Elolf, V. Bockermann, T. Gringel, M. Knauth, P. Dechent, and G. Helms, “Improved Visibility of the Subthalamic Nucleus on High-Resolution Stereotactic MR Imaging by Added Susceptibility (T2*) Contrast Using Multiple Gradient Echoes,” *Am. J. Neuroradiol.*, vol. 28, no. 6, pp. 1093–1094, Jun. 2007, doi: 10.3174/ajnr.A0527.
[25] L. G. Remore *et al.*, “The role of SWI sequence during the preoperative targeting of the subthalamic nucleus for deep brain stimulation in Parkinson’s disease: A retrospective cohort study,” *World Neurosurg. X*, vol. 22, p. 100342, Apr. 2024, doi: 10.1016/j.wnsx.2024.100342.
[26] F. Hertel, A. Husch, G. Dooms, F. Bernard, and P. Gemmar, “Susceptibility-Weighted MRI for Deep Brain Stimulation: Potentials in Trajectory Planning,” *Stereotact. Funct. Neurosurg.*, vol. 93, no. 5, pp. 303–308, 2015, doi: 10.1159/000433445.
[27] K. Yu *et al.*, “Visualization of subthalamic nucleus on susceptibility weighted imaging and the verification of accuracy by microelectrode recording,” *Front. Hum. Neurosci.*, vol. 19, p. 1559549, May 2025, doi: 10.3389/fnhum.2025.1559549.
[28] Y. J. Heo *et al.*, “Three-dimensional fluid-attenuated inversion recovery sequence for visualisation of subthalamic nucleus for deep brain stimulation in Parkinson’s disease,” *Neuroradiology*, vol. 57, no. 9, pp. 929–935, Sep. 2015, doi: 10.1007/s00234-015-1555-z.
[29] B. S. Succop, C. Zamora, D. A. Roque, E. Hadar, B. Kessler, and C. Quinsey, “Day one postoperative MRI findings following electrode placement for deep brain stimulation: analysis of a large case series,” *Front. Neurol.*, vol. 14, Dec. 2023, doi: 10.3389/fneur.2023.1253241.
[30] A. Boutet *et al.*, “Functional MRI Safety and Artifacts during Deep Brain Stimulation: Experience in 102 Patients,” *Radiology*, vol. 293, no. 1, pp. 174–183, Oct. 2019, doi: 10.1148/radiol.2019190546.
[31] A. Boutet *et al.*, “Improving Safety of MRI in Patients with Deep Brain Stimulation Devices,” *Radiology*, vol. 296, no. 2, pp. 250–262, Aug. 2020, doi: 10.1148/radiol.2020192291.
[32] N. B. Nuzov *et al.*, “Artifacts Can Be Deceiving: The Actual Location of Deep Brain Stimulation Electrodes Differs from the Artifact Seen on Magnetic Resonance Images,” *Stereotact. Funct. Neurosurg.*, vol. 101, no. 1, pp. 47–59, 2023, doi: 10.1159/000526877.
[33] A. Husch and F. Hertel, “DBS imaging methods II: Electrode localization,” in *Connectomic Deep Brain Stimulation*, Elsevier, 2022, pp. 127–146. doi: 10.1016/B978-0-12-821861-7.00004-X.
[34] N. I. Kremer *et al.*, “Accuracy of Intraoperative Computed Tomography in Deep Brain Stimulation—A Prospective Noninferiority Study,” *Neuromodulation Technol. Neural Interface*, vol. 22, no. 4, pp. 472–477, Jun. 2019, doi: 10.1111/ner.12918.
[35] Y. Nagayama *et al.*, “Metal Artifact Reduction in Head CT Performed for Patients with Deep Brain Stimulation Devices: Effectiveness of a Single-Energy Metal Artifact Reduction Algorithm,” *Am. J. Neuroradiol.*, vol. 41, no. 2, pp. 231–237, Feb. 2020, doi: 10.3174/ajnr.A6375.
[36] E. Atlı, S. A. Uyanık, U. Öğüşlü, H. Çevik Cenkeri, B. Yılmaz, and B. Gümüş, “Radiation doses from head, neck, chest and abdominal CT examinations: an institutional dose report,” *Diagn. Interv. Radiol.*, vol. 27, no. 1, pp. 147–151, Jan. 2021, doi: 10.5152/dir.2020.19560.
[37] T. A. Jaffe, J. K. Hoang, T. T. Yoshizumi, G. Toncheva, C. Lowry, and C. Ravin, “Radiation Dose for Routine Clinical Adult Brain CT: Variability on Different Scanners at One Institution,” *Am. J. Roentgenol.*, vol. 195, no. 2, pp. 433–438, Aug. 2010, doi: 10.2214/AJR.09.3957.
[38] J. Xia, P. He, X. Cai, D. Zhang, and N. Xie, “Magnetic resonance and computed tomography image fusion technology in patients with Parkinson’s disease after deep brain stimulation,” *J. Neurol. Sci.*, vol. 381, pp. 250–255, Oct. 2017, doi: 10.1016/j.jns.2017.08.3267.
[39] M. Shin, M. F. Penholate, J.-P. Lefaucheur, J.-M. Gurruchaga, P. Brugieres, and J.-P. Nguyen, “Assessing Accuracy of the Magnetic Resonance Imaging-Computed Tomography Fusion Images to Evaluate the Electrode

Downloaded from http://karger.com/sfn/article-pdf/doi/10.1159/000553009/4547863/000553009.pdf by guest on 08 July 2026

Positions in Subthalamic Nucleus After Deep-Brain Stimulation," *Neurosurgery*, vol. 66, no. 6, pp. 1193–1202, Jun. 2010, doi: 10.1227/01.NEU.0000369190.46510.42.
[40] J. F. Burke, D. Tanzillo, P. A. Starr, D. A. Lim, and P. S. Larson, "CT and MRI Image Fusion Error: An Analysis of Co-Registration Error Using Commercially Available Deep Brain Stimulation Surgical Planning Software," *Stereotact. Funct. Neurosurg.*, vol. 99, no. 3, pp. 196–202, 2021, doi: 10.1159/000511114.
[41] J. Engelhardt, D. Guehl, N. Damon-Perrière, O. Branchard, P. Burbaud, and E. Cuny, "Localization of Deep Brain Stimulation Electrode by Image Registration Is Software Dependent: A Comparative Study between Four Widely Used Software Programs," *Stereotact. Funct. Neurosurg.*, vol. 96, no. 6, pp. 364–369, 2018, doi: 10.1159/000494982.
[42] M. Luo, S. Narasimhan, P. S. Larson, A. J. Martin, P. E. Konrad, and M. I. Miga, "Impact of brain shift on neural pathways in deep brain stimulation: a preliminary analysis via multi-physics finite element models," *J. Neural Eng.*, vol. 18, no. 5, p. 056009, Oct. 2021, doi: 10.1088/1741-2552/abf066.
[43] K. Chee *et al.*, "Brain Shift during Staged Deep Brain Stimulation for Movement Disorders," *Stereotact. Funct. Neurosurg.*, vol. 102, no. 2, pp. 83–92, 2024, doi: 10.1159/000535197.
[44] C. Neudorfer *et al.*, "Lead-DBS v3.0: Mapping deep brain stimulation effects to local anatomy and global networks," *NeuroImage*, vol. 268, Mar. 2023, doi: 10.1016/j.neuroimage.2023.119862.
[45] A. Horn and A. A. Kühn, "Lead-DBS: A toolbox for deep brain stimulation electrode localizations and visualizations," *Neuroimage*, vol. 107, pp. 127–135, 2015, doi: 10.1016/j.neuroimage.2014.12.002.
[46] A. Horn *et al.*, "Lead-DBS v2: Towards a comprehensive pipeline for deep brain stimulation imaging," *Neuroimage*, vol. 184, pp. 293–316, 2019, doi: 10.1016/j.neuroimage.2018.08.068.
[47] A. Lasica *et al.*, "Precision of post-operative localization of deep brain stimulation electrodes," *Sci. Rep.*, vol. 15, no. 1, 2025, doi: 10.1038/s41598-025-01449-6.
[48] A. M. Noecker *et al.*, "StimVision v2: Examples and Applications in Subthalamic Deep Brain Stimulation for Parkinson's Disease," *Neuromodulation*, vol. 24, no. 2, pp. 248–258, Feb. 2021, doi: 10.1111/ner.13350.
[49] A. Husch, M. V. Petersen, P. Gemmar, J. Goncalves, and F. Hertel, "PaCER - A fully automated method for electrode trajectory and contact reconstruction in deep brain stimulation," *NeuroImage Clin.*, vol. 17, pp. 80–89, Oct. 2017, doi: 10.1016/j.nicl.2017.10.004.
[50] A. G. Yearley, M. Chua, A. Horn, G. R. Cosgrove, and J. D. Rolston, "Deep Brain Stimulation Lead Localization Variability Comparing Intraoperative MRI Versus Postoperative Computed Tomography," *Oper. Neurosurg. Hagerstown Md*, vol. 25, no. 5, pp. 441–448, Nov. 2023, doi: 10.1227/ons.0000000000000849.
[51] A. M. Noecker *et al.*, "StimVision v2: Examples and Applications in Subthalamic Deep Brain Stimulation for Parkinson's Disease," *Neuromodulation J. Int. Neuromodulation Soc.*, vol. 24, no. 2, pp. 248–258, Feb. 2021, doi: 10.1111/ner.13350.
[52] R. Reese *et al.*, "Combining ultrasound and microelectrode recordings for postoperative localization of subthalamic electrodes in Parkinson's disease," *Clin. Neurophysiol.*, vol. 156, pp. 196–206, 2023, doi: 10.1016/j.clinph.2023.11.001.
[53] A. Husch, M. V. Petersen, P. Gemmar, J. Goncalves, N. Sunde, and F. Hertel, "Post-operative deep brain stimulation assessment: Automatic data integration and report generation," *Brain Stimulat.*, vol. 11, no. 4, pp. 863–866, Jul. 2018, doi: 10.1016/j.brs.2018.01.031.
[54] T. A. Dembek *et al.*, "Probabilistic sweet spots predict motor outcome for deep brain stimulation in Parkinson disease," *Ann. Neurol.*, vol. 86, no. 4, pp. 527–538, Oct. 2019, doi: 10.1002/ana.25567.
[55] M. Koivu, A. Huotarinen, F. Scheperjans, A. Laakso, R. Kivisaari, and E. Pekkonen, "Motor outcome and electrode location in deep brain stimulation in Parkinson's disease," *Brain Behav.*, vol. 8, no. 7, p. e01003, Jul. 2018, doi: 10.1002/brb3.1003.
[56] A. Askari, B. J. Zhu, X. Lyu, K. L. Chou, and P. G. Patil, "Characterization and localization of upper and lower extremity motor improvements in STN DBS for Parkinson's disease," *Parkinsonism Relat. Disord.*, vol. 94, pp. 84–88, Jan. 2022, doi: 10.1016/j.parkreldis.2021.11.036.
[57] L. Rigon *et al.*, "Concordance between imaging and clinical based STN-DBS programming improves motor outcomes of directional stimulation in Parkinson's disease," *J. Park. Dis.*, vol. 15, no. 2, pp. 409–420, Mar. 2025, doi: 10.1177/1877718X241305725.
[58] V. Krishna *et al.*, "Connectivity-based selection of optimal deep brain stimulation contacts: A feasibility study," *Ann. Clin. Transl. Neurol.*, vol. 6, no. 7, pp. 1142–1150, Jul. 2019, doi: 10.1002/acn3.784.

Downloaded from http://karger.com/sfn/article-pdf/doi/10.1159/000553009/4547863/000553009.pdf by guest on 08 July 2026

[59] L. Verlaat *et al.*, “7-Tesla Magnetic Resonance Imaging Scanning in Deep Brain Stimulation for Parkinson’s Disease: Improving Visualization of the Dorsolateral Subthalamic Nucleus,” *Mov. Disord. Clin. Pract.*, vol. 11, no. 4, pp. 373–380, Apr. 2024, doi: 10.1002/mdc3.13982.
[60] J. Waldthaler *et al.*, “Imaging-based programming of subthalamic nucleus deep brain stimulation in Parkinson’s disease,” *Brain Stimulat.*, vol. 14, no. 5, pp. 1109–1117, Sep. 2021, doi: 10.1016/j.brs.2021.07.064.
[61] S. W. Hong, P. D. Dao, K. W. Chang, H. H. Jung, and J. W. Chang, “Minimizing Hemorrhage Complications in Deep Brain Stimulation Surgery - The Impact of Imaging Modalities and Trajectory Planning,” *J. Korean Neurosurg. Soc.*, vol. 68, no. 5, pp. 600–608, Sep. 2025, doi: 10.3340/jkns.2024.0198.
[62] P. Pezeshkian, A. A. F. DeSalles, A. Gorgulho, E. Behnke, D. McArthur, and A. Bari, “Accuracy of Frame-Based Stereotactic Magnetic Resonance Imaging vs Frame-Based Stereotactic Head Computed Tomography Fused With Recent Magnetic Resonance Imaging for Postimplantation Deep Brain Stimulator Lead Localization,” *Neurosurgery*, vol. 69, no. 6, pp. 1299–1306, Dec. 2011, doi: 10.1227/NEU.0b013e31822b7069.
[63] Y. Li *et al.*, “Mapping Motor Pathways in Parkinson’s Disease Patients with Subthalamic Deep Brain Stimulator: A Diffusion MRI Tractography Study,” *Neurol. Ther.*, vol. 11, no. 2, pp. 659–677, Jun. 2022, doi: 10.1007/s40120-022-00331-1.
[64] P.-F. D’Haese, S. Pallavaram, P. E. Konrad, J. Neimat, J. M. Fitzpatrick, and B. M. Dawant, “Clinical Accuracy of a Customized Stereotactic Platform for Deep Brain Stimulation after Accounting for Brain Shift,” *Stereotact. Funct. Neurosurg.*, vol. 88, no. 2, pp. 81–87, 2010, doi: 10.1159/000271823.
[65] C. Brimley and A. Kershenovich, “Deep brain stimulation lead migration in a child secondary to osteogenesis at the burr hole site,” *Interdiscip. Neurosurg.*, vol. 12, pp. 27–29, Jun. 2018, doi: 10.1016/j.inat.2017.09.009.
[66] V. Vedam-Mai *et al.*, “Deep Brain Stimulation associated gliosis: A post-mortem study,” *Parkinsonism Relat. Disord.*, vol. 54, pp. 51–55, Sep. 2018, doi: 10.1016/j.parkreldis.2018.04.009.
[67] P. J. Slotty, M. A. Kamp, C. Wille, T. M. Kinfe, H. J. Steiger, and J. Vesper, “The impact of brain shift in deep brain stimulation surgery: observation and obviation,” *Acta Neurochir. (Wien)*, vol. 154, no. 11, pp. 2063–2068, Nov. 2012, doi: 10.1007/s00701-012-1478-y.
[68] T. Morishita *et al.*, “Postoperative lead migration in deep brain stimulation surgery: Incidence, risk factors, and clinical impact,” *Plos One*, vol. 12, no. 9, 2017, doi: 10.1371/journal.pone.0183711.
[69] V. A. Coenen and M. Reisert, “DTI for brain targeting: Diffusion weighted imaging fiber tractography—Assisted deep brain stimulation,” 2021, pp. 47–67. doi: 10.1016/bs.irn.2021.07.001.
[70] N. Rajamani *et al.*, “Deep brain stimulation of symptom-specific networks in Parkinson’s disease,” *Nat. Commun.*, vol. 15, no. 1, p. 4662, May 2024, doi: 10.1038/s41467-024-48731-1.
[71] S. Abe *et al.*, “Diffusion tractography predicts Deep Brain Stimulation evoked potential amplitude and delay,” Apr. 13, 2024, *medRxiv*. doi: 10.1101/2024.04.11.24305627.
[72] K. Kamagata *et al.*, “Advancements in Diffusion MRI Tractography for Neurosurgery,” *Invest. Radiol.*, vol. 59, no. 1, pp. 13–25, Jan. 2024, doi: 10.1097/RLI.0000000000001015.
[73] D. Deuter *et al.*, “How accurate is probabilistic tractography when used to predict the ‘sweet spot’ in deep brain stimulation? Mind the gap!,” *Acta Neurochir. (Wien)*, vol. 167, no. 1, p. 305, Dec. 2025, doi: 10.1007/s00701-025-06719-w.
[74] J. Gerhardt *et al.*, “Retrospective distortion correction of diffusion tensor imaging data by semi-elastic image fusion – Evaluation by means of anatomical landmarks,” *Clin. Neurol. Neurosurg.*, vol. 183, p. 105387, Aug. 2019, doi: 10.1016/j.clineuro.2019.105387.
[75] S. Pujol *et al.*, “The DTI Challenge: Towards Standardized Evaluation of Diffusion Tensor Imaging Tractography for Neurosurgery,” *J. Neuroimaging Off. J. Am. Soc. Neuroimaging*, vol. 25, no. 6, pp. 875–882, Nov. 2015, doi: 10.1111/jon.12283.
[76] E. Calabrese, “Diffusion Tractography in Deep Brain Stimulation Surgery: A Review,” *Front. Neuroanat.*, vol. 10, p. 45, May 2016, doi: 10.3389/fnana.2016.00045.
[77] J. K. Wong, E. H. Middlebrooks, S. S. Grewal, L. Almeida, C. W. Hess, and M. S. Okun, “A Comprehensive Review of Brain Connectomics and Imaging to Improve Deep Brain Stimulation Outcomes,” *Mov. Disord. Off. J. Mov. Disord. Soc.*, vol. 35, no. 5, pp. 741–751, May 2020, doi: 10.1002/mds.28045.
[78] C. He, F. Zhang, L. Li, C. Jiang, and L. Li, “Measurement of Lead Localization Accuracy Based on Magnetic Resonance Imaging,” *Front. Neurosci.*, vol. 15, Dec. 2021, doi: 10.3389/fnins.2021.632822.

Downloaded from http://karger.com/sfn/article-pdf/doi/10.1159/000553009/4547863/000553009.pdf by guest on 08 July 2026

[79] M. Milchenko *et al.*, “ESM-CT: a precise method for localization of DBS electrodes in CT images,” *J. Neurosci. Methods*, vol. 308, pp. 366–376, Oct. 2018, doi: 10.1016/j.jneumeth.2018.09.009.
[80] B. Bhusal *et al.*, “Safety and image quality at 7T MRI for deep brain stimulation systems: Ex vivo study with lead-only and full-systems,” *PLOS ONE*, vol. 16, no. 9, p. e0257077, Sep. 2021, doi: 10.1371/journal.pone.0257077.
[81] R. Patriat *et al.*, “Individualized tractography-based parcellation of the globus pallidus pars interna using 7T MRI in movement disorder patients prior to DBS surgery,” *Neuroimage*, vol. 178, pp. 198–209, 2018, doi: 10.1016/j.neuroimage.2018.05.048.
[82] J. Qiu *et al.*, “Deep Learning and fMRI-Based Pipeline for Optimization of Deep Brain Stimulation During Parkinson’s Disease Treatment: Toward Rapid Semi-Automated Stimulation Optimization,” *IEEE J. Transl. Eng. Health Med.*, vol. 12, pp. 589–599, 2024, doi: 10.1109/JTEHM.2024.3448392.
[83] A.-S. Rolland *et al.*, “The Use of Image Guided Programming to Improve Deep Brain Stimulation Workflows with Directional Leads in Parkinson’s Disease,” *J. Park. Dis.*, vol. 14, no. 1, pp. 111–119, 2024, doi: 10.3233/JPD-225126.
[84] S. Glowinsky, Z. Israel, S. Heymann, and H. Bergman, “Divide and Conquer: Automatic Detection of the Thalamus to Empower DBS Physiological Navigation to the Subthalamic Region,” *IEEE Trans. Neural Syst. Rehabil. Eng.*, vol. 33, pp. 2672–2683, 2025, doi: 10.1109/TNSRE.2025.3582777.
[85] J. T. Boonstra and B. Genç, “Neuroimaging in deep brain stimulation: Bridging technical progress with clinical practice,” *Deep Brain Stimul.*, vol. 10, pp. 41–49, Nov. 2025, doi: 10.1016/j.jdbs.2025.08.001.
[86] J. Roediger *et al.*, “Automated deep brain stimulation programming based on electrode location: a randomised, crossover trial using a data-driven algorithm,” *Lancet Digit. Health*, vol. 5, no. 2, pp. e59–e70, Feb. 2023, doi: 10.1016/S2589-7500(22)00214-X.

Accepted Manuscript

Downloaded from http://karger.com/sfn/article-pdf/doi/10.1159/000553009/4547863/000553009.pdf by guest on 08 July 2026

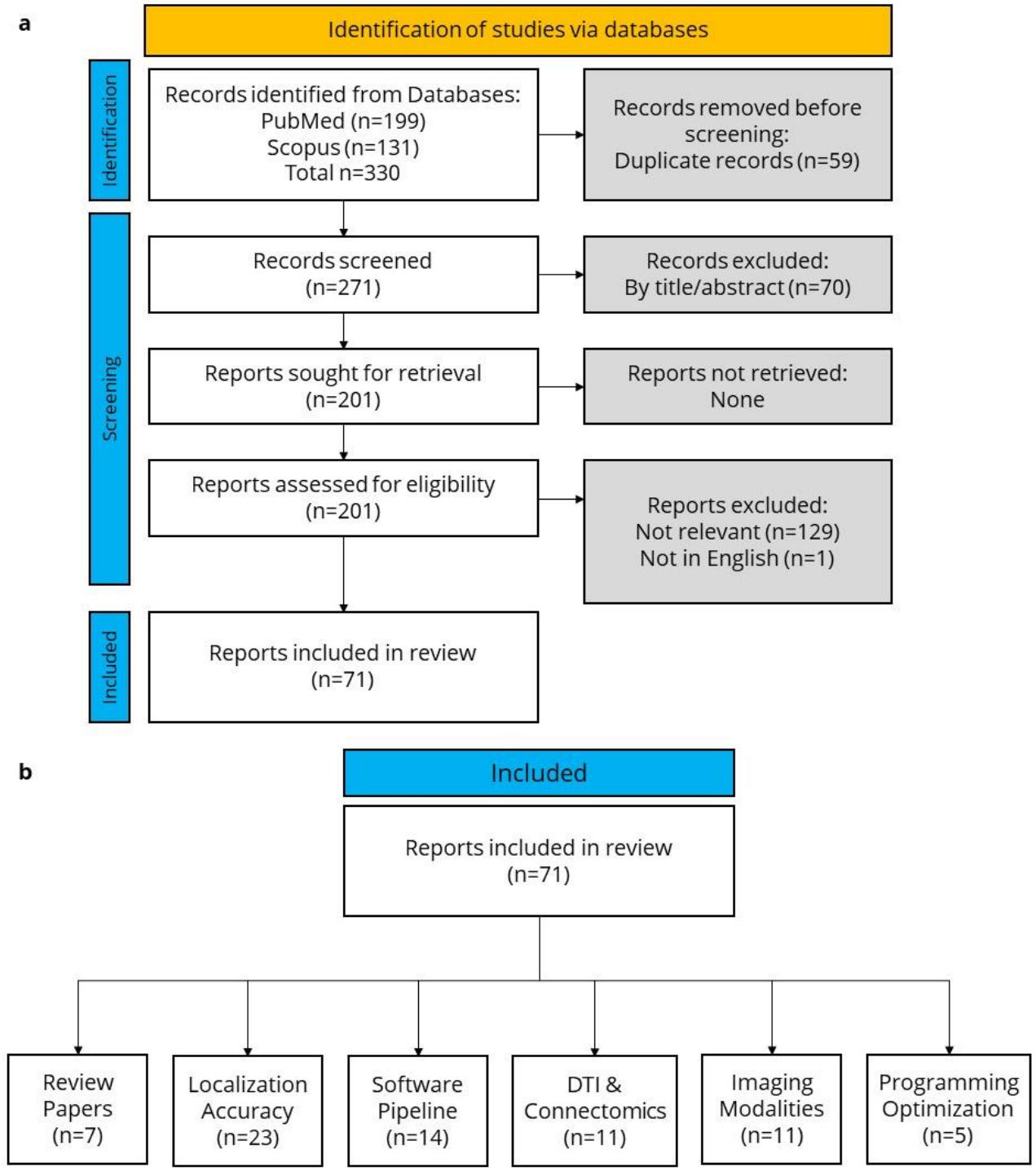
Figure Legends

Fig. 1. (a) PRISMA 2020 flow diagram for this literature review search and (b) the thematic distribution.

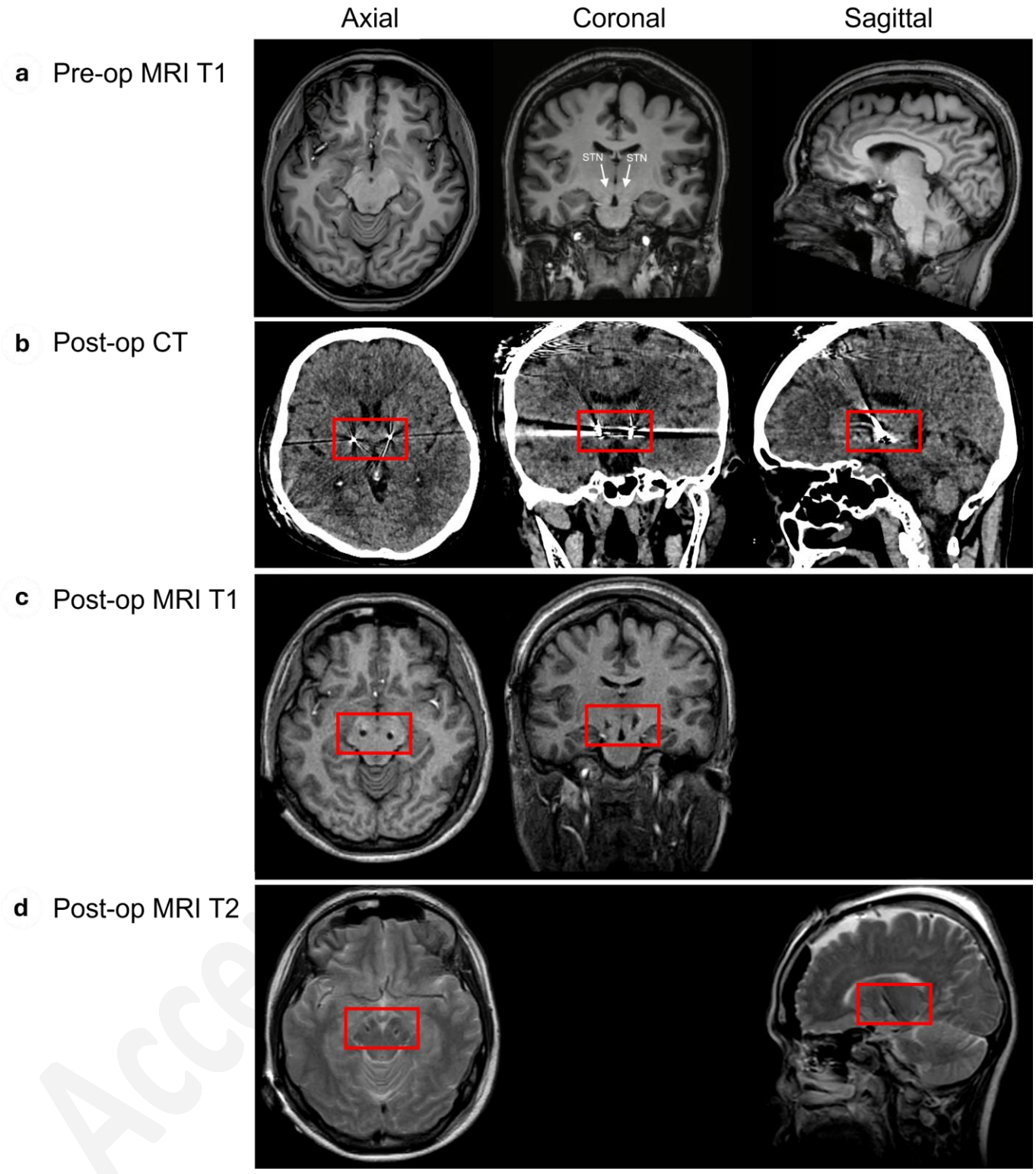
Fig. 2. Representative post-operative imaging examples from DBS patients. Columns show axial, coronal, and sagittal views. (a) Pre-operative T1-weighted MRI indicating the common DBS target, the subthalamic nucleus (STN); (b) post-operative CT highlighting DBS electrodes as bright hyperdense structures with associated streak artefacts; (c) post-operative T1-weighted MRI; and (d) post-operative T2-weighted MRI, where electrodes appear as dark signal voids. Red rectangles indicate the regions containing the DBS electrodes in each slice.

Accepted Manuscript

Downloaded from http://karger.com/sfn/article-pdf/doi/10.1159/000553009/4547863/000553009.pdf by guest on 08 July 2026



Downloaded from http://karger.com/sfn/article-pdf/doi/10.1159/000553009/4547863/000553009.pdf by guest on 08 July 2026



Downloaded from http://karger.com/sfn/article-pdf/doi/10.1159/000553009/4547863/000553009.pdf by guest on 08 July 2026

Table 1. Inclusion and exclusion criteria

Inclusion criteria	**Exclusion criteria**
Peer-reviewed journal articles	Animal or phantom studies
Human studies involving PD patients who underwent DBS implantation	Articles addressing DBS for non-PD indications only
Use of post-operative imaging for electrode localization, verification, or programming support	Studies focused exclusively on pre-operative planning or intra-operative targeting without post-operative imaging
Articles published in English	Studies focused solely on: • Surgical technique • Anesthesia • Electrophysiology without imaging • Non-imaging clinical outcomes such as cognition, gait, psychiatric effects, or quality of life • Ablative procedures and non-DBS interventions

Accepted Manuscript

Downloaded from http://karger.com/sfn/article-pdf/doi/10.1159/000553009/4547863/000553009.pdf by guest on 08 July 2026

Table 2. Previous studies listed with their acquisition parameters of post-operative imaging, timepoints and localization techniques.

Post-op Imaging Modality	Study (first author, publication year)	Key Acquisition Parameters	Timepoints	Localization Technique / Software Used
MRI	Succop et al. (2023) [29]	1.5 T MRI; 3D T1-MPRAGE, T2-FLAIR, T1/T2 GRE	1 day	Visual inspection of electrode artifact position
MRI	Lasica et al. (2025) [47]	1.5–3 T MRI; 3D T1-MPRAGE; voxel 0.45 × 0.45 × 0.9 mm	≥ 3 months	Lead-DBS, SureTune 4™, Brainlab Elements™
MRI + CT	Li et al. (2021) [23]	CT: voxel ~0.65 × 0.65 × 0.63 mm; MRI: 1.5 T, T1-MPRAGE, T2-FSE, ME-GRE	CT: ≤ 1 week; MRI: during hospitalization	Quantitative Susceptibility Mapping (QSM)
MRI + CT	Yearley et al. (2023) [50]	CT: 1 mm slices; MRI: 3 T T1-MPRAGE, 1 mm slices	MRI: immediate; CT: 1–2 days	Brainlab Elements™ Image Fusion
MRI + CT	Kremer et al. (2019) [35]	CT: voxel 0.49 × 0.49 × 0.5 mm; MRI: 1.5 T, voxel 0.72 × 0.72 × 2.2 mm	CT: immediate; MRI: 24–72 h	Brainlab iPlan 3.6
MRI + CT	Xu et al. (2023) [52]	CT: 0.63 mm slices; MRI: 3 T T1/T2	CT: immediate; MRI: 2 days	Lead-DBS, Surgical Planning System (rigid)
CT	Morishita et al. (2017) [53]	CT: voxel 0.49 × 0.49 × 1.25 mm	Immediate; 4-6 weeks	Rigid registration
CT	Chapelle et al. (2021) [54]	CT: voxel 0.49 × 0.49 × 0.63 mm	Immediate	Rigid co-registration; automatic thresholding
CT	Milchenko et al. (2018) [55]	CT: in-plane ~0.5 mm, slice 1 mm	Immediate;months later	Semi-automated ESM-CT
CT	Engelhardt et al. (2018) [41]	CT: <1 mm slice thickness	3 months	Manual lead tracing
CT	Lauro et al. (2016) [56]	CT: 1 mm slice thickness	Immediate	DBSproc pipeline
CT	Geevarghese et al. (2016) [57]	CT: voxel 0.5 × 0.5 × 1.25 mm	Immediate	Neuroinspire (Renishaw plc)
CT	Husch et al. (2018) [58]	CT: 1 mm slice thickness	Immediate	PaCER algorithm
CT + Ultrasound	Reese et al. (2023) [59]	CT: 1 mm slices; TCS: 1–5 MHz sector probe	CT: < 24 h; TCS: ≥ 3 months	Brainlab Elements™ fusion

Accepted Manuscript

Downloaded from http://karger.com/sfn/article-pdf/doi/10.1159/000553009/4547863/000553009.pdf by guest on 08 July 2026